Influence of the Grammage of Cardboard on its Damage Behavior in Impact Tests

Ulrike Kaeppeler[1,2*], Philipp Johst[3], Dimitrij Seibert[3], Robert Böhm[3], Lutz Engisch[1,2]

1 Leipzig University of Applied Sciences (HTWK Leipzig), Faculty of Computer Science and Media, Karl-Liebknecht-Straße 132, Leipzig 04277 Germany
2 iP[3] Leipzig – Institute for Printing, Processing and Packaging Leipzig, Karl-Liebknecht-Straße 132, Leipzig 04277 Germany
3 Leipzig University of Applied Sciences (HTWK Leipzig), Faculty of Engineering, Karl-Liebknecht-Straße 132, Leipzig 04277 Germany

* Corresponding author: ulrike.kaeppeler@htwk-leipzig.de

Abstract

The protection of goods is ensured by packaging. External influences can damage the packaging from outside, but the goods themselves can also damage the packaging from inside. Therefore, the selection of material is crucial. To enable an appropriate decision, it is important to understand the behavior of the material under impact stresses. In this study, it was examined how cardboard behaves under impact loading. Small impactors with different energies were shot at the material and the resulting mean impact diameter of the damage was determined. Two materials of different grammages were investigated. It was found that the damage behavior of the material corresponds with the grammage of the material.

1. Introduction

Cardboard is a commonly used packaging material, especially for sustainable packaging solutions. Typically, a multi-layer cardboard material is used. Cardboard has a complex fiber structure, usually consisting of wood fibers, fillers and a coating (Ek et al., 2009; Haslach, 2000). During manufacturing, the wood fibers are oriented in a preferred fiber direction, which, in combination with drying stresses, results in a strong anisotropy of the material (Niskanen, 2012). The associated variety of parameters leads to a complex material characterization.

Hydrogen bonds effectively connect the fibers in the structure. The hydrogen bonding force depends on the distance between the positive and negative potential allocation. The hydrogen bonds are only effective at short distances and are much weaker than a covalent bond (factor 15 to 30). When the fiber structure is stretched or punctured, the distance between the fibers increases, causing the fiber structure to break. Furthermore, the fibers themselves can break, but this requires more energy than the separation of the hydrogen bonds (Hüttermann, 2011; Käppeler, 2019; Neufingerl, 2016).

An impact is generally perpendicular to the material surface and leads to failure-relevant stresses in the thickness direction of the test specimen (Hornig, 2017). The present investigations are related to a study carried out by JOHST ET AL. (Johst et al., 2023). They conducted impact tests in which an impactor was shot perpendicular at the cardboard surface. The impactor hit the cardboard material. By varying the pressure, different kinetic energies of the impactor were generated. It was explored which damage phenomena occur at different impact energies and how they can be classified. Two different

cardboard materials were compared that exhibited the same damage phenomena. However, the materials' damage behavior differed in relation to impactor kinetic energies. It was hypothesized that this could be due to the different grammage of the materials. The underlying factor affecting the damage behavior could not be clearly confirmed by JOHST ET AL. (Johst et al., 2023) because two different materials with dissimilar grammage and fiber composition were used.

In this study, it is assumed that the damage behavior corresponds with the grammage of the material. In line with the findings of BIVAINIS AND JANKAUSKAS (Bivainis & Jankauskas, 2015), it will be examined whether these correlations found for corrugated board can be transferred to cardboard.

2. Experimental

2.1 Materials

Based on the experimental setup introduced by JOHST ET AL. two cardboard materials with similar composition were investigated. Two typical cardboards for e.g. folding boxes were used. According to Figure 1, both materials have the same layer structure. The material has a three-layer-fiber construction of chemical pulp (bleached sulphate pulp). It is double-coated on the top side and has a layer of light coating on the bottom side (Stora Enso, 2022).

The materials differ only in their grammage. The reference material, which was also used in the experiments by JOHST ET AL., has a grammage of 330 g/m^2 and will be designated A-330 in the following. The reference material has a grammage of 230 g/m^2 and will be named by C-230.

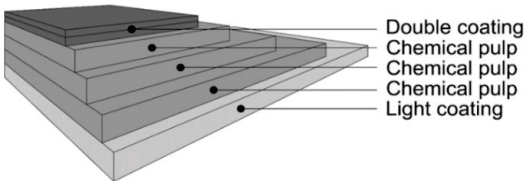

Figure 1: Layer composition of material A-330 and material C-230

The materials were stored for 48 hours in standard atmosphere (23 °C and 50 % +/- 2 % humidity) according to ISO 187 (2022) (Beuth Verlag, 2023). The thickness of both materials was measured following DIN EN ISO 534 (2012) (Beuth Verlag, 2012) with a thickness tester (Frank Dickenmesser, Frank-PTI GmbH, Birkenau, Germany). The thickness of material A-330 and material C-230 is about 401 µm and 259 µm, respectively. For the impact tests, the samples were cut into specimens with a width of 100 mm and a length of 100 mm, taking into account the fiber direction.

2.2 Experimental setup – Multiple-Impact-Test-Rig

The effect of impact loads on the cardboard material was investigated experimentally using a Multiple-Impact-Test-Rig (Mehrfach-Impact-Prüfstand, Hegewald & Peschke, Nossen, Germany). Figure 2 shows the experimental setup.

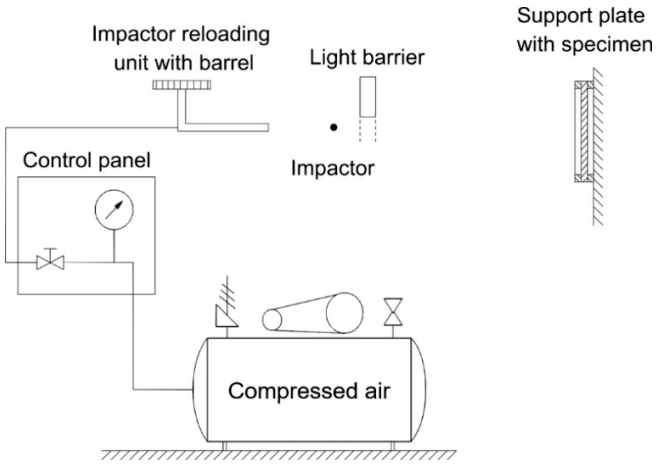

Figure 2: Experimental setup of Multiple-Impact-Test-Rig. Figure 2 is republished from Johst et al. (2023) with permission from the authors.

The test-rig enables a circular impactor to be accelerated in a barrel to a required velocity with compressed air. An impactor with a diameter of 4 mm and a mass of 0.26 * 10^{-3} kg was used for the experiments. The velocity of the impactor is adjustable with a control panel and is measured by a light barrier. Using the measured velocity v in m/s and the known mass m in kg of the impactor, the kinetic energy E in J can be determined with Eq.1.

$$E = \frac{1}{2} * m * v^2 \quad (1)$$

Due to the material composition, the specimens were aligned at the same position in the same preferred fiber direction in a support plate. The impact load caused by kinetic energy of the impactor was applied on the double coating side (see Figure 1) of the specimen.

Preliminary tests with material C-230 showed that permanent damage to the specimens is caused starting at a pressure of 0.03 MPa. From a pressure of 0.09 MPa, the damage pattern remained unchanged. Based on this knowledge, the pressure settings in the experiments were defined. Table 1 summarizes the number of all tests performed for materials C-230 and A-330 (Johst et al. 2023). At least 18 impacts were examined for all pressure settings of both materials.

Table 1: Experimental Settings of the Parameters Pressure, Number of Impacts, Mean Velocity of the impactor, and the Resulting Mean Kinetic Energy of the Impactor (values of material A-330 taken from Johst et al. 2023)

Settings	**Material A-330**							
Pressure in MPa	0.05	0.08	0.09	0.10	0.11	0.12	0.15	0.20
Number of Impacts	20	19	20	18	20	20	18	20
Velocity v in m/s*	18.77	24.59	26.25	27.25	29.28	30.56	33.09	38.24
Kinetic Energy E in J*	0.046	0.079	0.090	0.097	0.112	0.122	0.143	0.191
	Material C-230							
Pressure in MPa	0.03	0.04	0.045	0.05	0.055	0.06	0.07	0.08	0.09
Number of Impacts	20	20	20	20	20	20	20	20	19
Velocity v in m/s*	13.30	16.17	17.10	18.61	19.61	20.57	22.53	24.18	26.46
Kinetic Energy E in J*	0.023	0.034	0.038	0.045	0.050	0.055	0.066	0.076	0.091
*These parameters represent the mean values of the performed impacts									

2.3 Digital Analysis

A Keyence 3D macroscope (Keyence Germany GmbH, Neu Isenburg, Germany) was used to qualitatively and quantitatively examine the damage to the materials A-330 and C-230. First, the specimens were visually inspected. A screening was conducted to determine whether an imprint, cracking or a breakthrough occurred on the specimens. Consequently, a quantitative analysis was carried out by measuring the imprint diameter.

3. Results and discussion

3.1 Damage Phenomena

Figure 3 shows the comparison of the damage behavior of material C-230 (columns (a), (b), (c)) as well as material A-330 (column (d)). The top side of the material is shown in the upper row, and the bottom side of the material in the lower row. The height profiles of the samples are represented by color coding. In each case, the blue color indicates the lowest height in z-direction.

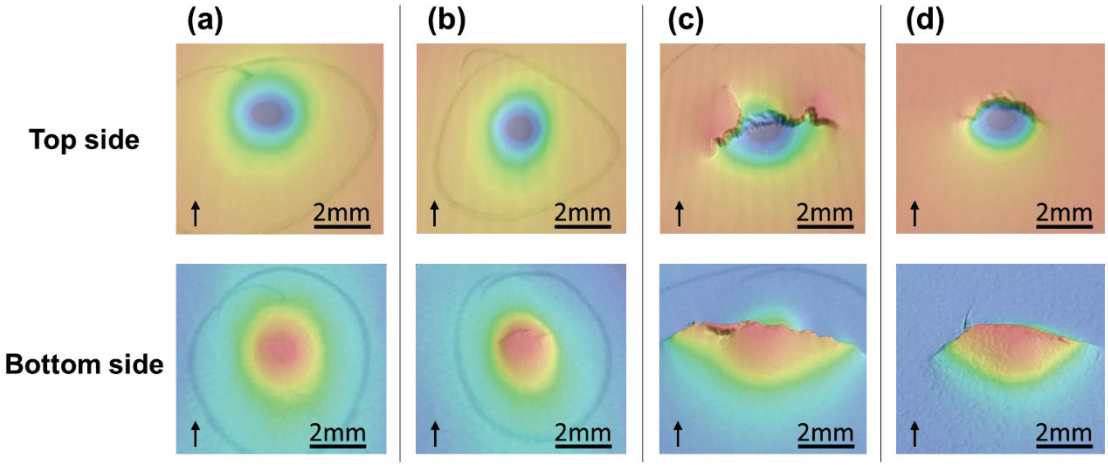

Figure 3: Comparison of damage behavior: Imprint, cracking and breakthrough for material C-230 ((a), (b), (c)) and material A-330 (d).

Column (a) shows an imprint of the impactor in the material C-230. It is only a plastic deformation without damage in the sense of a crack. In column (b) the cracking of the material is illustrated. The material begins to crack, but at this stage it has not yet completely torn through. This stage is shown in column (c) and is referred to as breakthrough. Compared to material C-230 (column (c)), the breakthrough of material A-330 is shown in column (d).

At the cracking stage, it is interesting to have a look at the upper side and the lower side of the material. The top side does not yet show any cracking, while the bottom side of the material already shows a crack. When the impactor hits the material, it is stretched in the z-direction. The layers on the top side and the bottom side of the material are stretched to different amounts (see Figure 4). The material experiences large strains on the outside (red marked surface), no strain in the middle of the material in the area of the neutral fiber, and kind of squeezing next to the impactor (green marked surface). This is comparable to the material behavior in bending tests. In the study shown here, the elongation of the material is multiaxial. Nevertheless, in this case, higher elongations

predominate on the bottom side, which is the side opposite to the impactor. This is the reason for the cracking on one side of the material.

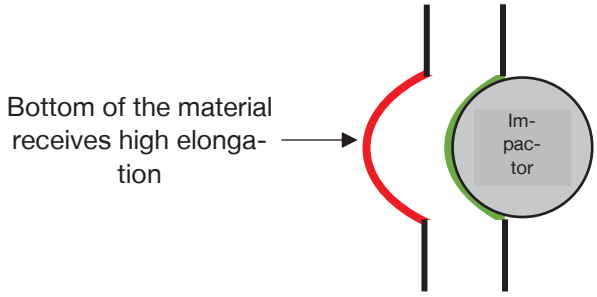

Figure 4: Different material elongation on the top and bottom side of the material

3.2 Comparing Mean Imprint Diameter

The results of the relationship between the mean imprint diameter and the energy level of material A-330 have been presented in previous studies (see (Johst et al., 2023)). The findings of material C-230 are given in Figure 5. They show an increase in the mean imprint diameter with increasing energy. The behavior of the two materials is comparable, but they differ noticeably in their energy levels.

The high variation of the values in the transition phase is obvious. In this phase, the specimens exhibit different damage phenomena (imprint, cracking or breakthrough), which can lead to considerable differences in the measurement of the mean imprint diameter from a horizontal and vertical measuring section.

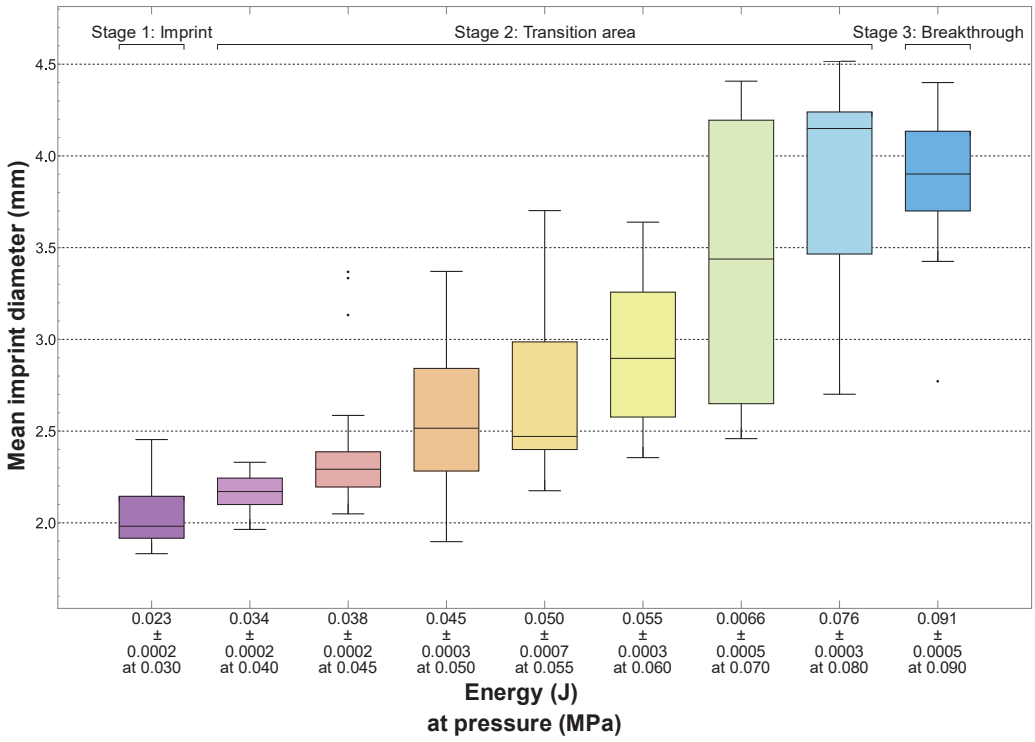

Figure 5: Boxplot for typical damage stages of material C-230

The resulted imprint diameter (D_{imp}) is ideally represented using a sigmoidal function, as given by Eq.2,

$$D_{imp} = f(E) = d + \frac{a-d}{\left(1+\left(\frac{E}{c}\right)^{b}\right)^{m}} \quad (2)$$

with a, b, c, d, and m as free variables. The approximated material specific parameters for material A-330 and material C-230 are listed in Table 2.

Table 2: Material Specific Parameters and Sigmoidal Function (values of material A-330 taken from Johst et al. 2023)

Variable	Material A–330	Material C-230
a	2.64	2.06
b	11.32	4.44
c	0.27	0.33
d	3.88	3.90
m	1719.78	1938.72
D_{imp}	$3.88 + \frac{2.64-3.88}{\left(1+\left(\frac{E}{0.27}\right)^{11.32}\right)^{1719.78}}$	$3.9 + \frac{2.06-3.9}{\left(1+\left(\frac{E}{0.33}\right)^{4.44}\right)^{1938.72}}$

Figure 6 shows the plots of D_{imp} for samples A-330 and C-230. The plot shows two interesting aspects: Material C-230 has a larger mean imprint diameter already at low energies, while material A-330 has a smaller imprint diameter at the same energy. The imprint diameter of material C-230 already increases markedly at lower energies, whereas the average imprint diameter of material A-330 becomes larger at energies estimated to be more than twice as high.

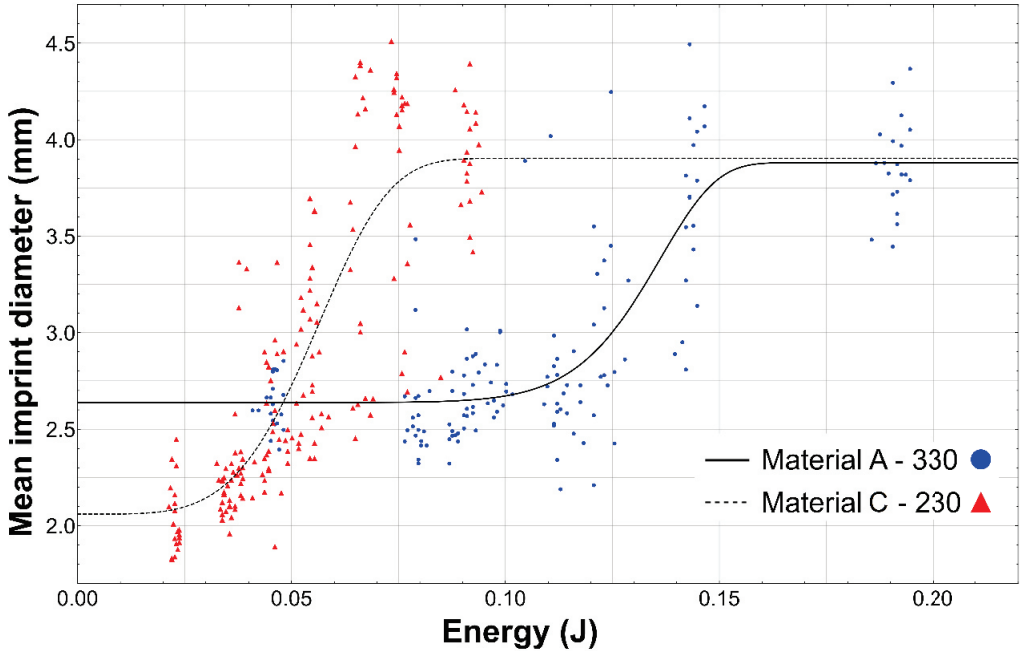

Figure 6: Comparison of the approximated sigmoidal functions for material A-330 and material C-230

Both materials reach their approximate maximum at an average imprint diameter of about 3.90 mm. This value is also expressed by the sigmoidal function of parameter d.

When comparing materials A-330 and C-330, it can be seen that parameter d is quite similar. For the material A-330 the parameter d = 3.88. This implies that the damage is roughly the same at high energies, but at lower energies, that means between 0.05 J and 0.15 j, the material C-230 has larger mean imprint diameters. This is due to the different grammage and therefore material thickness.

Material A-330 and material C-230 have the same composition, only their grammages differ. As a result, the materials have a similar density, while the thickness of the materials changes due to the change in grammage. With increasing thickness, the number of fiber layers stacked in the material increases. This also causes the quantity of hydrogen bonds to rise. When an impactor hits the surface of the material, more fiber layers and thus hydrogen bonds have to be punctured. This could be an explanation why less energy is required to induce the cracks and breakthroughs in material C-230 than in material A-330, since the grammage and thickness of material C-230 is lower compared to material A-330.

If the same energy is applied to the material, the impact load in material A-330 is mainly used for the initial destruction of the hydrogen bonds, whereas the energy in material C-230 is already sufficient for the complete destruction, which is shown by a breakthrough of the material. The destruction could be further investigated with other tests, for example a multiaxial strain test or a puncture test.

On the basis of these measurements, it can be concluded that the material with the higher grammage has better impact resistance. Thus, the damage behavior seems to correspond to the grammage.

4. Summary

The investigations presented in this paper focused mainly on the impact behavior of cardboard. It was shown that the grammage has a decisive influence on the impact resistance. The material with higher grammage showed a higher impact resistance than the material with lower grammage. Thus, these results are in accordance with the study of BIVAINIS AND JANKAUSKAS (Bivainis & Jankauskas, 2015). The findings can be used to develop a material model to numerically simulate the damage behavior.

Acknowledgement

Freistaat Sachsen

Dieses Forschungsvorhaben wird mitfinanziert durch Steuermittel auf der Grundlage des vom Sächsischen Landtag beschlossenen Haushaltes.

Sources

Beuth Verlag. (2012). *DIN EN ISO 534—Paper and board—Determination of thickness, density and specific volume*.

Beuth Verlag. (2023). *ISO 187—Paper, board and pulps – Standard atmosphere for conditioning and testing and procedure for monitoring the atmosphere and conditioning of samples* [International Organization for Standardization].

Bivainis, V., & Jankauskas, V. (2015). Impact of Corrugated Paperboard Structure on Puncture Resistance. *Materials Science*, *21*(1), 37–61. https://doi.org/10.5755/j01.ms.21.1.5713

Ek, M., Gellerstedt, G., & Henriksson, G. (2009). *Wood chemistry and wood biotechnology* (Bd. 1). de Gruyter.

Haslach, H. W. (2000). The Moisture and Rate-Dependent Mechanical Properties of Paper: A Review. *Mechanics of Time-Dependent Materials*, *4*(3), 169–210. https://doi.org/10.1023/A:1009833415827

Hornig, A. (2017). *Beitrag zur Analyse und Berechnung impactinduzierter Spallationsdelaminationen in Faserverbundwerkstoffen* [Dissertation]. Technische Universität Dresden.

Hüttermann, A. (2011). *Die Wasserstoffbrückenbindung: Eine Bindung fürs Leben*. Oldenbourg.

Johst, P., Kaeppeler, U., Seibert, D., Kucher, M., & Böhm, R. (2023). Investigation of different cardboard materials under impact loads. *BioResources*, *18*(1), 1933–1947. https://doi.org/10.15376/biores.18.1.1933-1947

Käppeler, U. (2019). *Anwendung physikalisch-chemischer Analysemethoden zur Charakterisierung von Faserverbunden* [Forschungsbericht]. Hochschule für Technik, Wirtschaft und Kultur Leipzig.

Neufingerl, F. (2016). *Chemie*. Jugend & Volk.

Niskanen, K. (Hrsg.). (2012). *Mechanics of Paper Products*. De Gruyter. https://doi.org/doi:10.1515/9783110254631

Stora Enso. (2022, September). *Ensocoat—Fully coated multilayer SBS board with light coated reverse*. https://www.storaenso.com/-/media/documents/download-center/documents/product-specifications/paperboard-materials/ensocoat-en-10012022.ashx